

Fig. 5 Tensile strength of geometrical similar samples with different heights

One obvious advantage of this model is that it can be applied on geometrical dissimilar specimens (Hu 2017). Fig. 6 shows the data of geometrical dissimilar samples with the same size and  $S/W$  but different  $\alpha$ -ratios. It is seen that the calculated  $f_t$  reaches the maximum value when  $\alpha \approx 0.25$ , and then decreases about 15% from  $\alpha = 0.3$  to  $\alpha = 0.4$ . The fitting tensile strength of samples with different  $\alpha$  is 216.0 MPa, which is perfectly coincided with the  $f_t$  value of all notched specimens, suggesting that the fracture model by Eq. (5) shows insensitive to size effect of different  $\alpha$ -ratios. Fig. 7 shows the data of samples with the same height and  $\alpha$ -ratio but two different  $S/W$  values. It is seen that the calculated  $f_t$  of samples with  $S/W=2.5$  is a little smaller than that of  $S/W=4$ . However, all of the data are located within the 96% reliability interval of all notched specimens, and their fitting tensile strength is very close, also verifying that the tensile strength calculated by Eq. (5) shows no significant size effect for specimens with  $S/W$  changes.

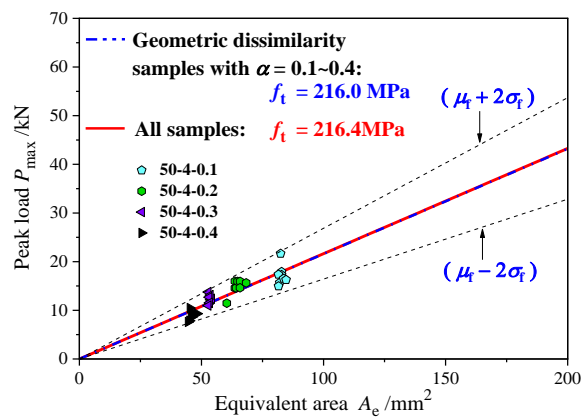


Fig. 6 Tensile strength of geometrical dissimilar samples with different  $\alpha$ -ratios

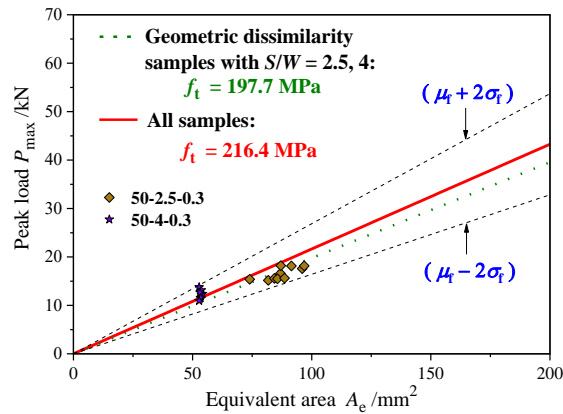


Fig.7 Tensile strength of geometrical dissimilar samples with S/W as 2.5 and 4

#### 4.2 Size effect analysis of un-notched samples

As explained in section 3.1, because of the material defects, un-notched samples of PSBL also have quasi-brittle fracture behavior, which produces obvious size effect result of the nominal tensile strength according to brittle strength theory. If the defect size on the sample surface is considered as the pre-cut notch length  $a_0$ , it can be determined by the plastic tensile strength which is obtained by the notched samples. Here,  $a_0$  of un-notched samples is calculated based on Eq. (5) with  $f_t$  decided as 216.7 MPa of notched samples. As shown in Fig. 8, Semi-logarithmic curves are used to fit the relation between surface defect size and specimen height, as  $a_0 = C_1 + C_2 \log W$  and

$a_e = C_3 + C_4 \log W$ .  $C_1$ ,  $C_2$ ,  $C_3$  and  $C_4$  are the coefficients.

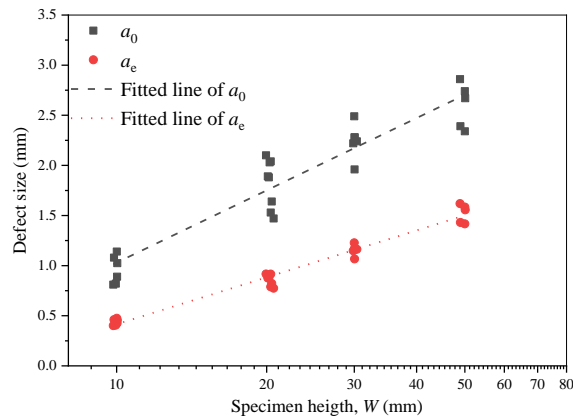


Fig. 8 Semi-logarithmic fitting between material defect size with sample height

With these fitting curves, the surface defect size of un-notched specimens are decided, which is considered as initial crack length  $a_0$ . And then, the tensile strength of these specimens is calculated according to Eq. (5). The results are shown in Fig. 9. It is seen that all the data of notched and un-notched samples distribute around the plastic

tensile strength  $f_t$ . So the brittle tensile strength of PSBL with different size can be decided by the size-independent plastic strength and the material defect size curve.

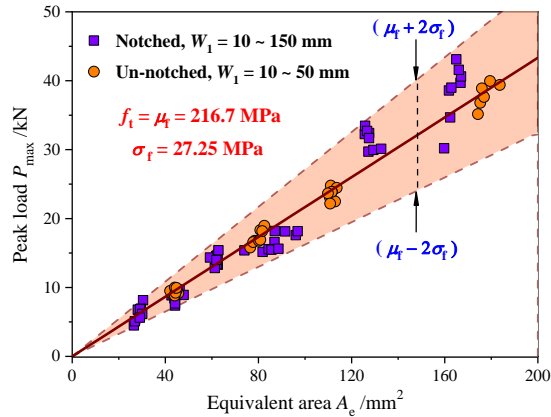


Fig. 9 Semi-logarithmic fitting between material defect size with sample height

## 5. CONCLUSION

The longitudinal tensile strength of PSBL has obvious size effect behavior according to the brittle strength theory, in that the test tensile strength decreases apparently with the increase of sample size, no matter notched or un-notched bending specimens. The reason for this size effect phenomenon is that the PSBL has quasi-brittle fracture character and the defects in front of the crack tip produce FPZ, which passives the crack tip and the causes strain-softening phenomenon during the fracture process. Because that FPZ size increases with structure size, the tested mechanical strength decreases with the increase of structure size

A simple model of tensile strength based on non-LEFM is introduced to analyse the size effect problem. With this model, the idea plastic tensile strength of PSBL is obtained, which is size-independent and suitable for both geometrical similar and dissimilar samples with different heights, span-to-height ratios and  $\alpha$ -ratios. Furthermore, the defect size is determined by the calculated plastic strength, and it is fitted by a semi-logarithmic relation with sample size. By this way, the solution for size effect phenomenon can be solved by such size-independent plastic strength and the material defect size curve.

## REFERENCES

- Bažant Z. (1984), "Size effect in blunt fracture: concrete, rock, metal", *J. Eng. Mech.*, ASCE, **110**, 518-35.  
 Bažant, Z. and Li, Z. (1995), "Modulus of rupture: size effect due to fracture initiation in

*The 2020 World Congress on  
The 2020 Structures Congress (Structures20)  
25-28, August, 2020, GECE, Seoul, Korea*

- boundary layer”, *J. Struct. Eng.*, ASCE, **121**(4), 739–746
- Bažant, Z. and Yu, Q. (2009), “Universal size effect law and effect of crack depth on quasi-brittle structure strength”, *J. Eng. Mech.*, ASCE, **135**, 78-84.
- Blank, L., Fink, G., Jockwer, R., et al. (2017) “Quasi-brittle fracture and size effect of glued laminated timber beams”, *Eur. J. Wood Wood Prod.*, **75**, 667-681.
- Hillerborg, A., Modeer, M., and Petersson, P. (1976), “Analysis of crack formation and crack growth in concrete by mean of fracture mechanics and finite elements”, *Cement Concrete Res.*, **6**, 773-782.
- Hu, X., Guan, J., Wang, Y., et al. (2017), “Comparison of boundary and size effect models based on new developments”, *Eng. Fract. Mech.*, **175**, 146-67.
- Huang, D., Bian, Y., Zhou, A., et al. (2015), “Experimental study on stress-strain relationships and failure mechanisms of parallel strand bamboo made from phyllostachys”, *Constr. Build. Mater.*, **77**, 130-138.
- Huang, D., Sheng, B., Shen, Y., et al. (2018), “An analytical solution for double cantilever beam based on elastic-plastic bilinear cohesive law: Analysis for mode I fracture of fibrous composites”, *Eng. Fract. Mech.*, **193**, 66-76.
- Liu, W., Hu, X., Yuan, B., et al. (2020), “Tensile strength model of bamboo scrimber by 3-p-b fracture test on the basis of non-LEFM”, *Compos. Sci. Technol.*, **198**, 108295.
- Liu, W., Yu, Y., Hu, X., et al. (2019), “Quasi-brittle fracture criterion of bamboo-based fiber composites in transverse direction based on boundary effect model”, *Compos. Struct.*, **220**, 347-354.
- Sharma, B., Gattoo, A., Bock, M., et al. (2015), “Engineered bamboo for structural applications”, *Constr. Build. Mater.*, **81**, 66-73.
- Verma, C., Sharma, N., Chariar, V., et al. (2014), “Comparative study of mechanical properties of bamboo laminate and their laminates with woods and wood based composites”, *Compos. Part B-Eng.*, **60**, 523-530.
- Yu, Y., Zhu, R., Wu, B., et al. (2015), “Fabrication, material properties, and application of bamboo scrimber”, *Wood Sci. Technol.*, **49**, 83-98.